The ReactorSTM: Atomically resolved scanning tunneling microscopy under high-pressure, high-temperature catalytic reaction conditions

C. T. Herbschleb, P. C. van der Tuijn, S. B. Roobol, V. Navarro, J. W. Bakker, Q. Liu, D. Stoltz, M. E. Cañas-Ventura, G. Verdoes, M. A. van Spronsen, M. Bergman, L. Crama, I. Taminiau, A. Ofitserov, G. J. C. van Baarle, and J. W. M. Frenken

Citation: Review of Scientific Instruments **85**, 083703 (2014); doi: 10.1063/1.4891811

View online: http://dx.doi.org/10.1063/1.4891811

View Table of Contents: http://aip.scitation.org/toc/rsi/85/8

Published by the American Institute of Physics

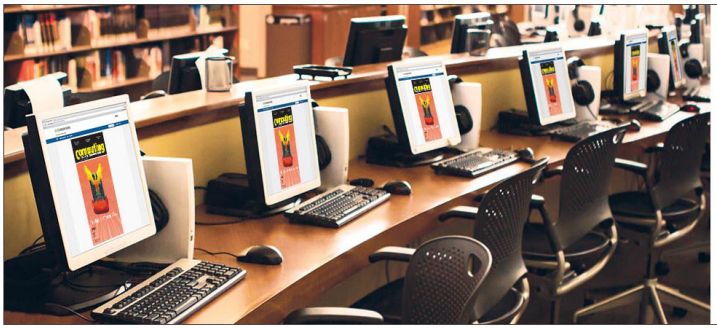

The ReactorSTM: Atomically resolved scanning tunneling microscopy under high-pressure, high-temperature catalytic reaction conditions

C. T. Herbschleb,[1,a)] P. C. van der Tuijn,[1] S. B. Roobol,[1] V. Navarro,[1] J. W. Bakker,[1] Q. Liu,[1,b)] D. Stoltz,[1,c)] M. E. Cañas-Ventura,[1,d)] G. Verdoes,[1,e)] M. A. van Spronsen,[1] M. Bergman,[1] L. Crama,[1] I. Taminiau,[1,f)] A. Ofitserov,[2] G. J. C. van Baarle,[2] and J. W. M. Frenken[1,g)]

[1]*Huygens-Kamerlingh Onnes Laboratory, Leiden University, P.O. box 9504, 2300 RA Leiden, The Netherlands*
[2]*Leiden Probe Microscopy B.V., J.H. Oortweg 21, 2333 CH Leiden, The Netherlands*

(Received 31 March 2014; accepted 21 July 2014; published online 15 August 2014)

To enable atomic-scale observations of model catalysts under conditions approaching those used by the chemical industry, we have developed a second generation, high-pressure, high-temperature scanning tunneling microscope (STM): the ReactorSTM. It consists of a compact STM scanner, of which the tip extends into a 0.5 ml reactor flow-cell, that is housed in a ultra-high vacuum (UHV) system. The STM can be operated from UHV to 6 bars and from room temperature up to 600 K. A gas mixing and analysis system optimized for fast response times allows us to directly correlate the surface structure observed by STM with reactivity measurements from a mass spectrometer. The *in situ* STM experiments can be combined with *ex situ* UHV sample preparation and analysis techniques, including ion bombardment, thin film deposition, low-energy electron diffraction and x-ray photoelectron spectroscopy. The performance of the instrument is demonstrated by atomically resolved images of Au(111) and atom-row resolution on Pt(110), both under high-pressure and high-temperature conditions. [http://dx.doi.org/10.1063/1.4891811]

I. INTRODUCTION

Much of our current knowledge of the precise mechanisms underlying chemical reactions at catalyst surfaces is derived from experiments under ultra-high vacuum (UHV) or high vacuum (HV) conditions. The discrepancy with respect to the typical working conditions of practical catalysts comes from the fact that many surface-sensitive techniques such as low-energy electron diffraction (LEED), Auger electron spectroscopy (AES), and X-ray photoelectron spectroscopy (XPS) cannot be combined easily with the environment to which a catalyst would normally be exposed, for example, in the three-way catalyst of a car or in catalytic processes in the petrochemical industry. Moreover, the UHV provides a clean and easily controllable environment for accurate experiments.[1,2] Although such low-pressure model studies have contributed extensively to our fundamental understanding of catalysts, recent investigations at high gas pressures have yielded new insights that go beyond the mere extrapolation of the low-pressure results.[3–6] This difference is often referred to as the "pressure gap."[7] Recently, several surface analysis techniques have been adapted to more realistic conditions. Examples are transmission electron microscopy (TEM),[8] surface X-ray diffraction (SXRD),[9] scanning tunneling microscopy (STM),[10–14] and atomic force microscopy (AFM).[15]

Scanning tunneling microscopy is one of the few atomically sensitive surface-science techniques that do not introduce fundamental problems or limitations when bridging the pressure gap. It can operate in the full range from UHV to high pressures of, e.g., 1 bar and beyond, and from cryogenic temperatures to temperatures well above 1000 K.[16,17] With its capability to image surfaces with atomic resolution, the STM holds the promise to determine the detailed dependence of the structure of model catalyst surfaces on various gas environments, to identify the active sites for catalytic reactions and to elucidate the role of possible promoters, all under the relevant, high-pressure, high-temperature conditions of the catalytic processes of interest. The weakness of the local tip-surface interaction provides confidence that in most cases this interaction will not significantly affect the structure and the properties of the catalyst. These advantageous properties of the technique go hand in hand with a demanding combination of technical difficulties. The main difficulty is the imaging stability of the instrument in terms of the drift and noise resulting from temperature and pressure variations and the presence of a gas flow. In addition, to desire to detect reaction products in the gas mixture adds additional constraints on the volume of the high-pressure cell versus the surface area of the model catalyst sample.

a)Present address: ASM Europe BV, Versterkerstraat 8, 1322 AP Almere, The Netherlands.
b)Present address: Carbon-Biotechnology Ltd., Xiangyun Road No. 6, 203000 Wujin Jingfa district, Changzhou, Jiangsu, China.
c)Present address: Royal Institute of Technology (KTH), Electrum 229, Isafjordsgatan 22, 16440 Kista, Sweden.
d)Present address: Evonik Industries AG, Paul-Baumann-Straße 1, 45772 Marl, Germany.
e)Present address: Christaan van der Klaauw Astronomical Watches, Businesspark Friesland-West 47, 8447 SL Heerenveen, The Netherlands.
f)Present address: Infinite Potential Laboratories, 485 Wes Graham Way, Ontario N2L 0A7, Canada.
g)Author to whom correspondence should be addressed. Electronic mail: frenken@physics.leidenuniv.nl. Present address: Advanced Research Center for Nanolithography, P.O. Box 41883, 1009 DB Amsterdam, The Netherlands.

In this paper we present the design and performance of the ReactorSTM. The setup combines an STM, partly integrated in a small flow cell, with a UHV system that is equipped with standard surface preparation techniques, such as ion bombardment and metal deposition. The ReactorSTM enables us to study the surface structure of a catalyst in combination with simultaneous mass spectrometry and thereby directly correlate structural changes with chemical activity. We start this paper with a discussion of the concept and the specifications of the instrument, followed by a description of the actual design and performance.

II. CONCEPT

Figure 1 summarizes the concept of the ReactorSTM. It consists of a small reactor volume with inert walls, inside a UHV system. The reactor is connected to two thin gas lines, one serving as the gas inlet and the other as the exhaust. The inlet is connected to a gas system which controls the flow, mixing ratio and pressure of the reactant gasses. The exhaust is connected to a mass spectrometer for analysis of the composition of the gas flow that leaves the reactor. Of the scanning tunneling microscope, only the STM tip and the tip holder are exposed to the gasses inside the reactor. Two flexible o-rings seal off the reactor volume from the UHV. The lower o-ring separates the reactor on the lower side from all other STM components, such as the piezo element that is used to actuate the motion of the tip; these components stay in UHV, while the pressure in the reactor can be as high as several bar. In this way, the reactor volume is kept small, which lowers the detection limit of reaction products, makes the refresh rate of the gas in the reactor high and the response time to changes in the reactivity short. It also ensures that most of the vulnerable components of the STM are not exposed to high pressures of aggressive gasses. The upper o-ring, against which the sample surface is pressed, is used to seal the reactor on the upper side from the surrounding UHV environment. The sample is radiatively heated from the rear, i.e., the upper side.

The architecture of a small high-pressure cell inside a UHV system is radically different from early high-pressure STM designs,[11–13] in which a UHV chamber is backfilled with gas, and it goes significantly further than the current state of the art,[14] by keeping the piezo element outside of the high-pressure volume. This has important additional advantages leading to unequalled imaging performance, especially at elevated temperatures.

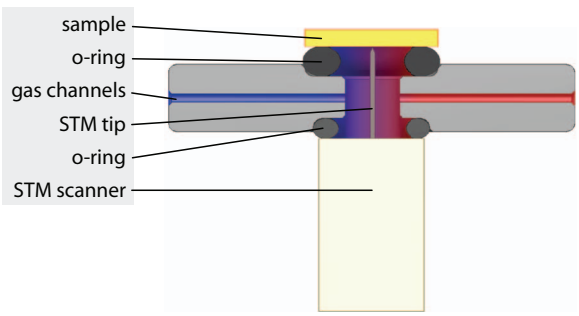

FIG. 1. Conceptual drawing of the ReactorSTM. The STM tip is contained within a small high-pressure volume, while the STM scanner is not exposed to the gasses. The sample forms one side of the reactor while the other reactor walls are chemically inert. Two polymer o-rings seal off the high-pressure volume from the UHV system around it.

First of all, this design avoids convective heat transport via the gas phase from the sample to the scanner. Small differences in temperature, for example, between the hot sample and the cooler piezo element, can result in significant convective motion in the gas. Test measurements for a typical STM configuration have shown this type of heat transport to be erratic and to change magnitude on a timescale of a few seconds. This resulted in severe, erratic drifting distortions in the STM images on the same timescale. Without the presence of gas around the piezo element, such distortions are avoided completely. In addition, the limited heat transport also minimizes the total heating power, thereby further reducing thermal drifting of the scanner. Without convection, the drift is not erratic in nature and can be coped with routinely. Finally, this design allows for a much smaller reaction volume, which reduces the residence time of the gas, needed to reach a measurable concentration of reaction products, which makes it possible to operate the reactor in flow rather than batch mode.

Similar to other high-pressure STM designs, this configuration makes it straightforward to combine the high-pressure experiments with UHV techniques. Ultrahigh vacuum is a prerequisite for high-quality sample preparation, involving ion sputtering, metal deposition, vacuum annealing, et cetera, and for the application of traditional, sensitive surface analysis techniques, such as low-energy electron diffraction (LEED), Auger electron spectroscopy (AES) and X-ray photoelectron spectroscopy (XPS). UHV is also important to avoid contamination of the freshly prepared samples during their transfer to the high-pressure environment. This naturally leads to a configuration with a high-pressure cell that can be sealed off inside a UHV system. We have chosen to combine all required functionalities into a multi-chamber UHV setup, of which one chamber contains the high-pressure cell, integrated with the STM.

III. SPECIFICATIONS

In order to approach industrial conditions during our STM measurements, we need to operate the STM with the sample surface exposed to a controllable gas flow at pressures beyond 1 bar. A meaningful time resolution in the reactivity measurements that matches high imaging rates, requires the gas flow to be high enough to refresh the reactor volume within a few seconds. For a small reactor, with a volume in the order of 1 ml, this requirement translates into a flow of typically 10 ml_n/min. In addition to high pressures, industrial conditions imply high temperatures. How high depends very much on the specific catalytic process at hand. The window of typical conditions starts at 400 K and runs up to much higher temperatures, such as 1000 K and above. Although we have developed a variable temperature (UHV) STM that routinely images surfaces at sample temperatures of 1000 K and above,[17] for the ReactorSTM we prioritize gas response times and accurate reactivity measurements over temperature range.

Therefore we limit ourselves to 600 K, a temperature that is achievable with elastomer seals, allowing a more compact design.

STM imaging with high resolution, resolving the atomic structure at a catalyst surface, requires a stable STM with a short mechanical loop between the tip and the specimen surface, an effective vibration isolation system, good temperature stability to suppress thermal drift, and a low electronic noise level. The total noise level should not exceed a fraction of the atomic corrugation, i.e., in the images it should typically remain below 0.01 nm, both along the surface plane and perpendicular to it. To image rapid processes at the surface, under reaction circumstances, high-speed scanning is also needed. Our target here is to acquire one image per second. In order to correlate the observed surface structure with measurements of the reaction rate, it is necessary to operate the STM simultaneously with a mass spectrometer, in our case a quadrupole mass spectrometer (QMS). The complete gas detection system should have a response time in the order of seconds. This involves leading part of the exhaust gas line of the reactor volume to the QMS without creating a large dead volume, and without influencing the control over pressure and flow in the reactor.

An integral part of the ReactorSTM is a dedicated gas handling system that produces gas flows through the reactor volume with flow rates corresponding to a residence time of gas in the reactor ranging from seconds to minutes, and, independently, a range of total pressures below and above 1 bar. In order to explore the effect of the gas composition, the gas system should make it possible to generate mixtures of gasses. We have chosen for mixtures of up to four gasses plus a carrier gas. For the investigation of the effect of composition, the gas system should be able to vary the mixing ratios over a wide range, for which we have chosen a maximum value of 100:1. Short response times require the volume of the gas system to be minimal. For the same reason, dead volumes cannot be tolerated. A very interesting type of measurement is to follow the response of the catalyst to a sharp pulse of a different gas composition. One of the requirements for such experiments in combination with the sensitive STM observations is that such pulses do not lead to significant variations in total flow and total pressure. Cleanliness of the gas composition makes it important that the entire gas system can be baked out, in our case to 343 K. Finally, the gas system should be fully computer controlled and interfaced with the STM control and data acquisition system, which is necessary for time synchronization purposes.

The requirements that directly affect the STM configuration can be summarized as follows:

- *Imaging resolution:* atomic resolution (z-resolution below 0.01 nm) on close-packed metal surfaces under high-pressure, high-temperature conditions, e.g., at 1 bar and 450 K.
- *Imaging rate:* 1 or more images per second (images of 256 × 256 pixels, e.g., 5 nm × 5 nm).
- *Gas pressure in the reactor:* beyond 1 bar.
- *Ratio between partial pressures of different gasses in gas mixture:* up to 100:1.
- *Refresh time constant gas mixture in reactor:* down to 5 s.
- *Gas flow rate through the reactor:* up to 10 ml_n/min.
- *Time delay for gas mixture between gas handling system and reactor:* less than 5 s.
- *Time delay for gas mixture between reactor and mass spectrometer:* less than 5 s.
- *Temperature range of the catalyst:* room temperature up to 600 K
- *Thermal drift:* below 1 μm/h (piezo range) in z-direction; below 50 nm/min along x,y.

IV. DESIGN

In this section we discuss the general architecture of the UHV system and provide a more detailed description of the ReactorSTM and gas handling system.

A. UHV system

Figure 2 shows the configuration of the UHV system. It consists of three chambers[18] separated by valves.[19] From left to right, these chambers are the XPS chamber, the preparation chamber, and the STM chamber. Sample holders can be placed in different positions and orientations in each of these chambers, required to face each of the installed preparation and analysis tools. The sample holders can be transported between the chambers by means of a rack and pinion transfer rod.[18] A sample load-lock system mounted on the XPS chamber makes it possible to quickly introduce and export sample holders without the need to break the main vacuum. Each of the three chambers is pumped separately by an ion pump in combination with a Ti sublimation pump.[20] Additionally, the

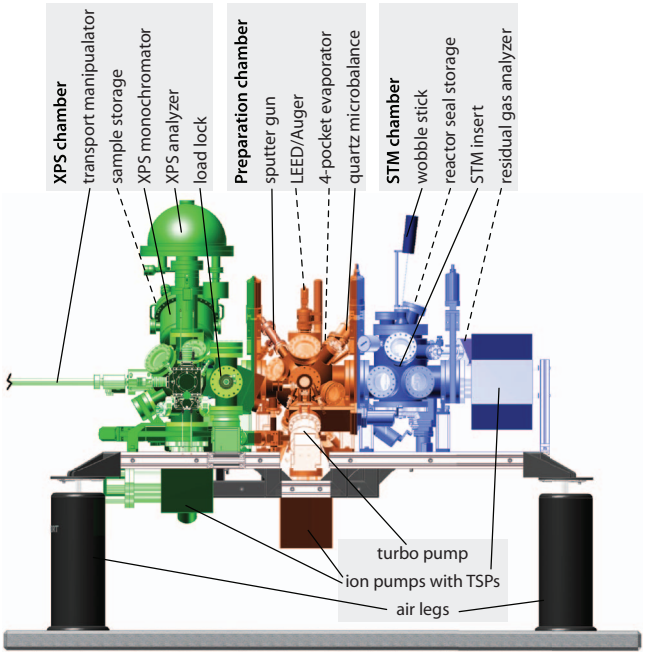

FIG. 2. Schematic drawing of the UHV system showing the three chambers with the equipment for sample preparation and characterization. Dashed lines point to components that are not visible.

preparation chamber is equipped with a chemically resistant turbo-molecular pump,[21] which is used to evacuate the system after it has been vented and to continuously pump the high gas flows that are sometimes required during preparation of model catalyst surfaces. To reach UHV, the vacuum system can be baked to 425 K, by means of two heating fans and a bake-out tent that encloses the entire system. During STM operation, the turbo-molecular pump is always off, in order to avoid the coupling of its mechanical vibrations into the STM. To minimize the influence of external mechanical vibrations, the entire, three-chamber combination is mounted on a stiff frame that is supported by air legs.[22]

The main component of the STM chamber is the high-pressure STM itself, which is mounted on the bottom flange, including all its electrical connections and gas lines. On the top flange of the chamber, a seal library has been installed together with a wobble stick. This combination makes it possible to easily replace the seal that separates the high pressure inside the reactor from the UHV of the STM chamber, as described in Sec. IV B.

The preparation chamber houses a manipulator, which can translate and rotate the sample surface, to face each of the instruments on the chamber. These include an ion gun[23] for sputter cleaning of the surface, an e-beam evaporator[24] for metal deposition, for example, to obtain thin metal films or supported nano-particles, and a combined LEED/AES system[25] for quick inspection of the periodicity, crystal quality, and cleanliness of the surface. A gas manifold with Ar, O_2, H_2, or other gasses is connected to the preparation chamber via automated all-metal leak valves.[26] Using a valve and separate pumping connection, the LEED/AES system can be sealed off from the rest of the preparation chamber, which is particularly useful during sample preparation steps that involve significant pressures of aggressive gasses, such as O_2 or H_2S.

The XPS chamber is dominated by the X-ray source and the hemispherical energy analyzer of the XPS setup,[27] which can be used for inspection of the surface chemical composition prior to and after high-pressure experiments. The chamber is made out of Mu-metal to shield the XPS from external magnetic fields. The chamber also contains a sample library that can store two additional sample holders.

B. STM configuration

Figure 3(a) shows a schematic cross section of the combination of the sample holder and the reactor with STM scanner. With the sample holder placed on the STM, a small, 0.5 ml reactor volume is defined. This reactor volume is sealed off from the surrounding UHV by two elastomer rings. The upper seal is clamped between the catalyst sample and the STM body. It is a custom-made Kalrez[28] ring that is vulcanized onto a stainless steel holder, which enables us to exchange these seals using a wobble stick without breaking the vacuum. The lower seal is a Viton O-ring between the STM body and the top part of the scan actuator. Both rings are chemically rather inert, especially the Kalrez, which is in direct contact with the active catalyst surface. The Kalrez seal is specified for operation up to 600 K and this limits the operating temperature of the STM.

The STM body is made out of Zerodur,[29] a type of glass that has a low thermal expansion coefficient, which minimizes the thermal drifting of the STM during temperature changes. An additional advantage of this material is that it is chemically inert, which is necessary since the upper surface of the STM body forms one of the walls of the high-pressure cell.

The hat-shaped sample is held in position in the sample holder by a molybdenum spring. It is electrically isolated from the other components of the sample holder. A filament, mounted behind the sample, enables sample heating either by thermal radiation or by electron bombardment. A sapphire shield thermally isolates the filament from the rest of the sample holder. A type K thermocouple is laser-spot-welded to the sample, for accurate temperature measurement. The sample holder has a 5-pin connector that provides separate

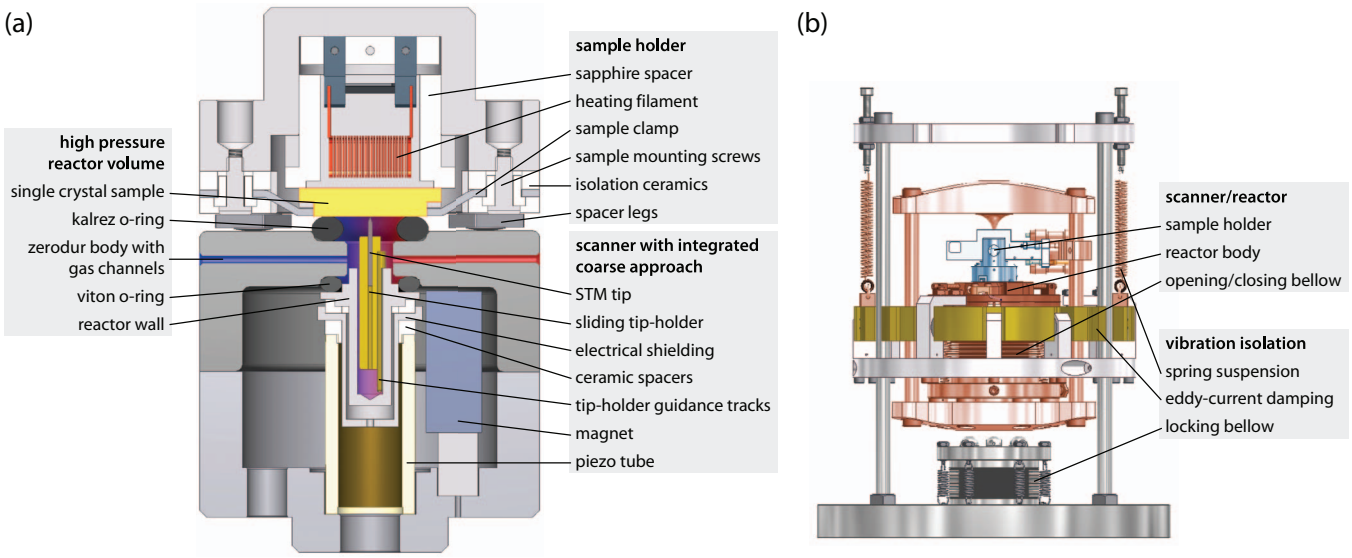

FIG. 3. Detailed schematic of (a) the scanner and reactor and (b) the insert with vibration isolation, mounted on a CF-200 flange.

contacts to the filament, the thermocouple and the sample. The latter connection is used either to ground the sample, e.g., for ion sputtering, electron bombardment, XPS, LEED, and AES, or to provide a bias voltage for STM and STS measurements. Two versions have been constructed of the sample holder body, one out of Zerodur[29] and the other out of Invar, a low-expansion steel. In both cases, a low-expansion material was used, again to minimize thermal drift. The brittleness of Zerodur established a practical disadvantage, which made us prefer the Invar version. Fortunately, XPS spectra acquired on samples clamped in the Invar holder did not indicate noticeable changes in the spectrum due to the magnetic character of the Invar.

The sample holder is strongly pressed against the top of the STM body, so that it makes hard mechanical contact via three adjustable screws. In this way a short and stiff mechanical loop is established between the sample and the tip, which is essential for high-quality STM imaging. After a sample has been mounted in its sample holder, the length of the three screws is adjusted such that with the screws in contact with the scanner body, the Kalrez ring is compressed to 80% of its original thickness. This situation provides a reliable, leak-tight seal, enabling to maintain UHV in the STM chamber, even when the reactor volume is exposed beyond atmospheric pressure.

Two thin silica-coated capillaries run up from gas feedthroughs on the bottom flange (see below) and connect to the reactor volume via channels in the Zerodur STM body. One is used as the supply line of gasses into the reactor; the other serves as the exhaust line.

A single piezotube is used for both the coarse approach and the fine scanning motion. The STM tip is clamped in a steel holder, which is pulled against two steel rails by a SmCo magnet[30] that is glued on a separate support. The three steel parts, tip holder, and rails are gold-plated in order to ensure chemical inertness and to optimize the stick-slip behavior of the holder along the rails (see below). The magnetic force, determined by the distance between the tip holder and the magnet, is tuned via the size, shape, and location of the magnet, in such a way that the maximum acceleration that can be generated along the length axis by the EBL2 piezo element[31] is high enough to overcome the static friction force between the tip holder and the rails. In this way, the same piezo element used for STM scanning is also used to inertially translate the tip holder up or down along the rails, which makes it possible to perform a controlled approach- or disengage motion over several mm distance. The electrical connection to the tip that is necessary to measure the tunneling current is established via the tip holder and the rails and the aluminum tube in which the rails are clamped. We have selected aluminum as the material for this tube, since this tube is in contact with the reactive gas mixture and aluminum is inert for the catalytic reactions under investigation. Electrical shielding is provided by an additional hat-shaped aluminum piece. The two aluminum parts are electrically isolated from each other and from the piezo tube by two insulating Macor[32] rings. The piezo element is glued to a titanium base, which has a thermal expansion coefficient that compensates the expansion of the piezo tube during temperature changes.

The backbone structure in Figure 3(b) is used to combine the complete STM assembly with vibration isolation and the necessary electrical connections and gas capillaries on a single CF-200 flange. In spite of its complexity, the STM assembly is a compact unit that is mounted relatively easily from below into the SPM chamber of the UHV system. The STM portal that holds the STM body, the Kalrez seal, and the sample holder, is suspended by a set of springs that is combined with an eddy current damping system, in order to isolate the STM from external, mechanical vibrations. The two silica-coated capillaries are each connected to a gas feedthrough on the bottom flange. Both are wound as soft springs around the portal to minimize coupling of external mechanical vibrations via the gas lines into the STM.

Two features are essential to facilitate easy and reliable transfer of sample holders into and out of the STM portal. First of all, during sample transfer activities, the spring suspension should be disarmed by mechanically locking the STM portal to the backbone structure. This makes it possible to exert forces on the portal for pushing in or pulling out sample holders. Second, the system should enable one to generate a force up to 100 N to mechanically press the sample and sample holder against the reactor body, thereby compressing the kalrez seal by 20% and closing the reactor volume with respect to the UHV chamber; also the opposite should be possible, pulling sample and sample holder away from the reactor body. Once the reactor is closed, it should remain closed, also when the STM portal is unlocked and suspended from the springs. These two actions are achieved by means of the controlled inflation of two bellows. When the upper bellow is inflated, the sample and sample holder are pressed against the reactor body and the reactor volume is sealed off from the surrounding UHV. When the lower bellow is inflated, the STM portal is locked to the backbone structure. The upper bellow is connected via a capillary to a gas feedthrough, and the lower one is directly connected to a feedthrough. The capillary of the upper bellow is again wound as around the portal, to minimize mechanical vibrations.

The STM is controlled by fast analog/digital SPM control electronics[33] capable of video-rate STM imaging.[34]

C. Gas supply and analysis system

As motivated above, a gas system was required that can mix various gasses over wide ranges in composition, with separate control over the gas flow rate of each individual component in the mixture and the total pressure of the gas flow with a short response time, in the order of a few seconds or less. The latter requirement necessitates a configuration with small total volume and without dead or badly refreshed gas volumes. Another requirement was that it should be possible that during STM imaging the partial gas pressures, flow rates and total pressure can be changed, without having to interrupt imaging. This means that no unwanted effects such as pressure bursts, with possible tip crash as result, can be tolerated. Fortunately, for applications in, e.g., gas chromatography (GC) and high-performance liquid chromatography, a wide range of components is commercially available with extremely low dead volumes, such as tubing, connection pieces, filters, and several

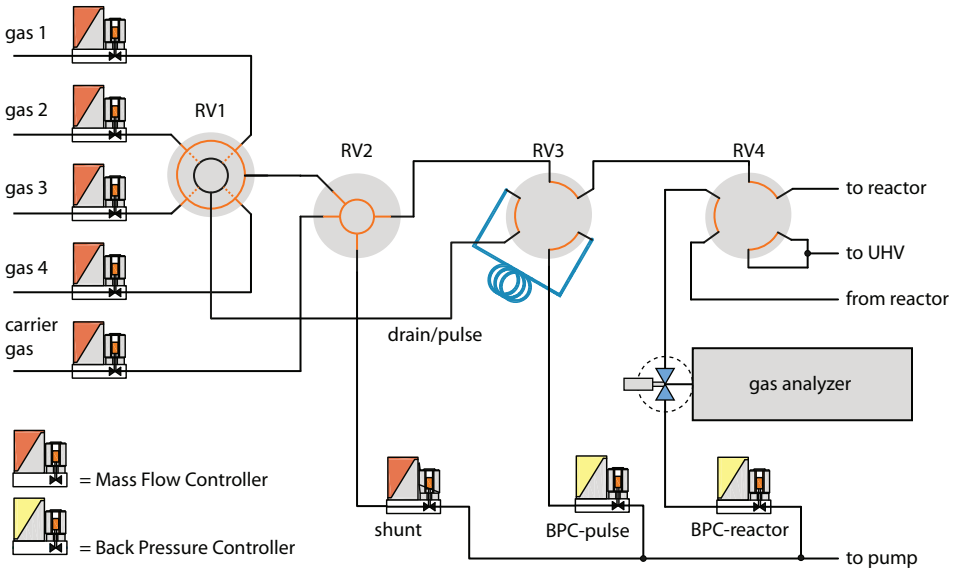

FIG. 4. Manifold for gas mixing and analysis. Up to four gasses plus a carrier gas can be mixed by a computer controlled manifold, consisting of rotating valves (RV1-4), several mass flow controllers (MFCs), and two back pressure controllers (BPCs). A continuous sampling gas analyzer[37] provides high time-resolution gas analysis.

types of valves, including rotating valves. In our gas system a special role is played by a custom-modified version of a GC valve. The crucial element is a rotor with a conical polymer surface that contains an engraved pattern. This rotor is pressed inside a metal body, to ensure a leak-tight seal. By rotation of the rotor the engraved pattern can be made to access and interconnect different channels, drilled in a symmetric, radial pattern in the metal body. This can be used to obtain different flow paths, depending on the rotor position. Note that it is possible to engrave the rotor such that no dead volume is enclosed in this valve at any time, also not in the channels that are not in use. For the specific needs of our gas system, we have produced rotors with several custom engraving patterns.

To separately control the composition, the flow rate, and the total pressure inside the reactor, we have employed a combination of mass flow controllers (MFCs) and back pressure controllers (BPCs) from Bronkhorst Hi-Tech[35] with a flow rate of 0–10 ml_n/min and pressure range of 0–6 bars, respectively.

In our gas system the outer diameter of the stainless steel tubing is chosen to be 1/16 in. The choice of the inner diameter of the tubing is a trade-off between very small volumes that would reduce the total internal volume of the system thereby optimizing the response time, and larger volumes to minimize the pressure drop over the gas lines for a given flow rate to reduce the difference in the pressure measured by the BPC and the actual pressure inside the reactor. We chose 0.5 mm inner diameter for the tubing between the MFCs and the reactor, since for that part of the system the response time is the most important parameter and a certain pressure drop between the MFCs and the reactor can be tolerated. For the section\ between the reactor and the BPC, the pressure drop should be minimal in order to relate the BPC reading to the reactor pressure; for this section of the tubing an inner diameter of 0.75 mm was chosen.

Using these components, we have adopted the architecture schematically shown in Figure 4. The high purity gases gas 1–4, in our implementation O_2, CO, NO, and H_2, are supplied from lecture bottles with reducing valves. To prevent particles from entering the gas system, particle filters are placed between the reducing valves and the MFCs. Each of the gasses flows through a MFC, which determines the flow rate of that gas. The rotating valve RV1 is the "mixing valve" and can select any combination of the maximally four gas flows that arrive at its input. The flow exiting the mixing valve and entering the "selector valve" (RV2) is the sum of the selected gas flows. The engraving pattern of the mixing valve is such that those gases that are not selected are not "stored" in the valve, but leaving the valve via the line indicated as "drain/pulse." Via the loop and the pulse BPC, the not selected gases are pumped away. The role of this BPC is crucial, since it allows one to, prior to the addition of a certain gas to the flow to the reactor, stabilize the flow pressure of that gas flow to match the current reactor pressure. After this stabilization, RV1 can be switched to add the extra gas flow to the reactor flow, without detrimental effects on the STM-imaging.

RV2 directs the flow via RV3 towards the STM reactor volume. The second output of RV2 is connected to the shunt MFC and enables one to split off a part of the flow by sending it via the shunt line to the pump. This makes it possible to reach extremely low flow rates through the reactor, without the need for extreme (and inaccurate) settings for the MFC's. A second inlet of RV2 is connected to a carrier gas MFC and allows for having very small partial pressures of a certain mixture in the reactor while still having a large total pressure. It also ensures that for very small flows of a mixture, a flow of carrier gas can be added to have a good response time to a change of settings.

Before the gas flows to the reactor, it passes the "pulse valve" (RV3). In addition to the regular gas flow from the selector, RV3 also receives input from the pulse/drain line,

connected to RV1, which it stores in a small gas loop with a total volume which is selected to be 0.5 ml, equal to the reactor volume. The pressure of the gas in that loop can be controlled by the "pulse BPC." In the orientation of RV3 shown in Figure 4, the gas flow from RV2 is passed down to RV4 and the not-selected gasses from RV1 are sent via the loop volume and the pulse BPC towards the pump. RV3 can be rotated rapidly into a position in which the extra volume of the gas loop is inserted into the flow path of the regular gas mixture. This generates a well-defined pulse of the gas that was initially stored in the loop. The configuration of this valve with the gas loop is such that, in case both the pulse and reactor BPC have the same set point, the pulse only provides a short variation in the gas composition, while it does not change the total pressure or the total gas flow. Therefore the pulse can be applied during STM imaging without having to retract the tip.

The final rotating valve, RV4, is a rotating 6-way valve that has two positions. The first position, shown in Figure 4, is for high-pressure STM experiments. In this position, the prepared mixture is directed towards the reactor. The flow exiting the reactor is sent via RV4 towards the gas analyzer. After passing by the gas analyzer, the flow is finally directed via RV4 towards a BPC that controls the reactor pressure independently from the total gas flow. The BPC is connected directly to the pump that generates the flow through the reactor. The two other connections of RV4 are connected to the main UHV chamber. In the second position of RV4, both the inlet and outlet lines of the reactor are connected to the UHV via RV4. This ensures that the sample is protected as good as possible from degassing of the capillaries and reactor wall when the reactor has been closed but no gas exposure is desired yet, for example, during coarse approach. Another role of the second position of RV4 is that it connects the gas stream leaving RV3 directly to the BPC of the reactor, via the gas analyzer. In this way the gas composition can be tested by QMS or GC analysis prior to exposing the sample to the gas. It also allows keeping the gas system clean by having always a flow through most of the lines, even when the reactor is open to the UHV.

The gas analyzer is placed before the BPC to make it independent of the varying flow impedance of the BPC. However this means that the analyzer must operate in the full pressure range of 0–6 bars and can only consume a small fraction of the gas flow. In addition, the requirement of at most 5 s delay between gas leaving the reactor and being analyzed places a tight restriction on the internal volume of the analyzer. A T100 gas analyzer[36] is used, which is based on a QMS. This analyzer has a 5 µl inlet volume and a typical gas consumption of less than 1 μl_n/min, and it is tunable for operation across the desired pressure range. If response time is not an issue for the experiment, then the internal volume of the analyzer is no longer restricted, and this system can be replaced by or complemented with any other gas analysis method, including gas chromatography and infrared spectroscopy.

All valves of the gas supply system are controlled by a PC. LabView and Python programs have been written to continuously log the valve settings and BPC/MFC read-outs. The Python software also allows programming of sequences of actions.

V. PERFORMANCE

In this section we present the essential aspects of the performance of the complete ReactorSTM setup. After a brief summary of the vacuum and gas flow behavior, we turn to the STM imaging performance under vacuum and high-pressure conditions, at room temperature and at elevated temperatures.

A. UHV system and gas manifold

The three chambers of the UHV system routinely reach a base pressure of in the range of 10^{-10} mbar after a bake-out of 48 h at 400 K. The operation of the bellows used to open and close the reactor and to lock the spring suspension system of the STM did not have any effect on the pressure in the UHV system. In practice, an absolute pressure of approximately 4 bars in the bellow that closes the reactor results in a sufficiently large closing force to compress the Kalrez seal and establish a rigid coupling between the surface of the Zerodur reactor body and the three adjustment legs on the sample holder. With that closing force, we can operate the reactor at pressures up to 6 bars, while the leak rate from the reactor into the UHV chamber typically results in a slight raise of pressure to the 10^{-9} mbar range. Eventually, after longer use, seals have been observed to degrade, leading to a modest increase of the UHV pressure when having high pressures inside the reactor.

The performance of the modified rotating GC valves over time was evaluated during use. After having been rotated a few hundred times, they were still found to exhibit a low leak rate in the order of 10^{-9} mbar l/s. Setting a new position of these rotating valves takes 0.1–1 s, depending on the travel the rotor has to make. The possible momentary interruption of the gas flows, caused by the rotation of the valve rotors, is sufficiently buffered by the volume of the gas lines and only modestly affects the STM imaging. The time response of the gas system is illustrated in Figure 5 by a typical time-trace of the gas analyzer during a CO oxidation experiment. In this experiment, we switched from a 50% CO flow to a 50% O_2

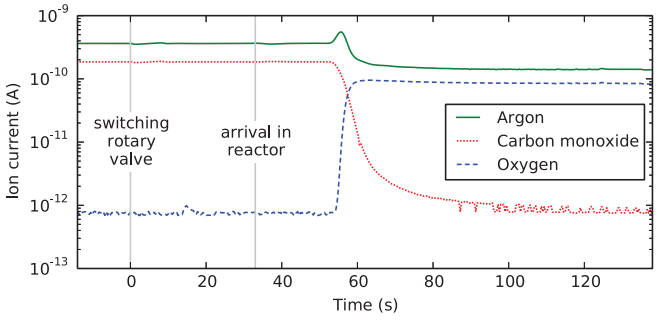

FIG. 5. Gas mixing response at 1 bar, 2 ml_n/min total flow, as detected by the mass spectrometer. Replacing CO by O_2 starting from a 1:1 mixture of Ar and CO, using rotary valve RV1 (Figure 4). The arrival of the gasses in the reactor at T = 33 s has been deduced from thermal drift in the STM images. The transition time of the O_2 introduction is 5 s. The spike in the Ar signal is an increase in partial pressure caused by the momentary interruption of the CO and O_2 flows during the movement of the rotary valve. Note that the Ar flow is not interrupted since it enters the manifold via RV2, neither is there an effect on the total pressure.

flow with argon as carrier gas at a pressure of 1 bar. At a modest flow of 2 ml_n/min, it takes 33 s for the gas to reach the reactor and another 20 s to reach the mass spectrometer. These delays scale linearly with flow, so an improvement of a factor 10 can easily be gained with higher flows. The switch from the O_2 to the CO atmosphere is completed within approximately 5 s, indicating the low intermixing of the gases in the gas lines, the reactor, and the sampling valve.

B. STM

A first series of test measurements was performed to establish the imaging resolution and high-speed performance of the STM in "UHV-mode." In this mode, the ReactorSTM is fully operational but we leave out the Kalrez seal between sample and reactor, so that the reactor is pumped via the UHV chamber. The presence or absence of this seal has no influence on the imaging performance, but makes a significant difference for the pressure to which the sample (and the tip) are exposed. Thus, the "UHV-mode" enables us to judge the imaging performance, unperturbed by gasses. Figure 6 demonstrates that the imaging resolution of the ReactorSTM is comparable to that of other, typical UHV-STM setups, i.e., not compromised by the special, high-pressure-flow-reactor configuration with the capillaries, the bellows, the Zerodur, and the stick-slip tip holder for coarse approach. Atomic resolution is obtained routinely, not only on graphite (panels (a) and (b)) but also on the close-packed Au(111) surface (panels (c) and (d)). The z-resolution is estimated to be 10 pm (panel (e)). Note that we have measured atomically resolved images at frame rates up to 4 images/s with only mild image distortions (panel (b)), which is favorable for acquiring movies of dynamic phenomena.

The thermal behavior of the ReactorSTM setup was characterized by ramping the sample temperature from 410 K to 460 K over the course of 3 h, while imaging the surface continuously with the STM. From the comparison of the images over this 3-h time window, we deduce that the average displacement was ∼25 nm/K parallel to the surface and ∼8 nm/K perpendicular to the surface. The lateral drift component was uniform and small enough to be accommodated comfortably by routine drift correction techniques and over the full 50 K temperature window, both drift components added up to no more than approximately one third of the full range of the piezo scanner.

The influence of the total reactor pressure on the STM imaging was explored by scanning the Au(111) surface while ramping the reactor pressure from 0 bar up to 3 bars and back to 0 bar. This resulted in reversible displacements below 300 nm parallel to the surface (i.e., below 100 nm/bar) and below 400 nm perpendicular to the surface (below 133 nm/bar). Over this wide pressure range, the mechanical distortions of the ReactorSTM setup are thus modest enough to remain well within the range of the piezo scanner.

The full performance of the ReactorSTM is illustrated in Figure 7, in which atomic resolution is demonstrated on Au(111) at a high sample temperature of 378 K and an O_2

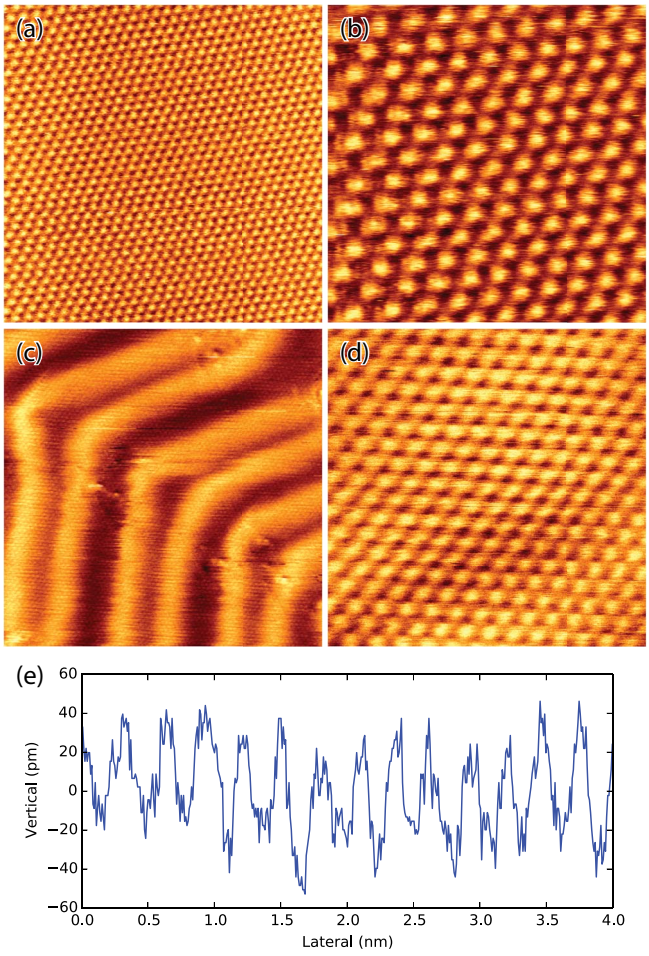

FIG. 6. Four atomically resolved STM images obtained with the ReactorSTM in "UHV mode" at room temperature. (a) and (b) Highly oriented pyrolithic graphite (HOPG), 8.0 nm × 8.0 nm (512 × 512 pixels) at 8.7 s/image, and 2.9 nm × 2.9 nm (512 × 512 pixels) at 2.6 s/image, both imaged with a tunneling voltage of $V_t = 0.40$ V and a tunneling current of $I_t = 0.46$ nA. (c) and (d) Au(111) surface, 23 nm × 23 nm (512 × 512 pixels, $V_t = 0.10$ V, $I_t = 0.12$ nA), and 4.6 nm × 4.6 nm (512 × 512 pixels, $V_t = 0.12$ V, $I_t = 0.10$ nA). The zig-zag pattern in (c), which is also present as a modulation in height and in lateral position in (d) is due to the well-known "herringbone reconstruction" on Au(111). (e) Height line from an atomically resolved Au(111) image, providing an estimate of the z-noise of 10 pm peak-to-peak for a bandwidth of 5 kHz.

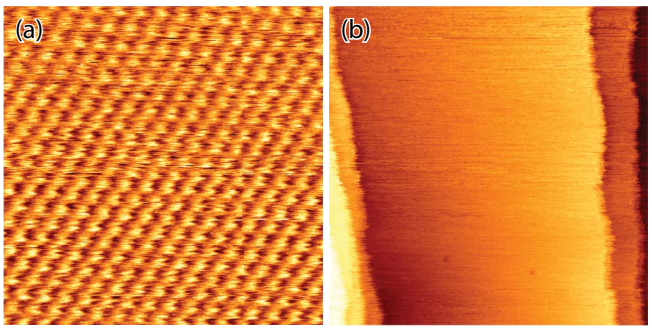

FIG. 7. Two STM images obtained with the ReactorSTM on Au(111) in a flow of 10 ml/min of O_2 at a pressure of 1.2 bars and at a sample temperature of 378 K. (a) Small-area image showing atomic resolution, 4.4 nm × 4.4 nm, taken with a tunneling voltage of $V_t = 0.22$ V and a tunneling current of $I_t = 0.20$ nA, corrected for drift by shearing the image horizontally over 21°, then cropped. (b) Larger-area image, $V_t = 0.24$ V, $I_t = 0.24$ nA, 75 nm × 75 nm, showing step fluctuations.

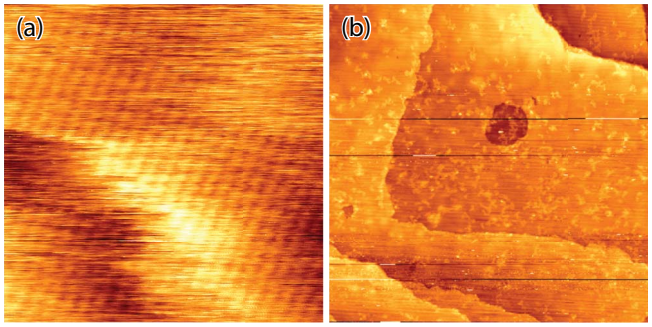

FIG. 8. Two STM images obtained with the ReactorSTM under high-pressure high-temperature conditions. (a) The Pt(110) surface, showing atomic rows with a vague signature of the individual atoms, 7.5 nm × 7.5 nm, imaged in a flow of 1 bar of CO at a sample temperature of 433 K, imaged with a tunneling voltage of $V_t = -0.04$ V and a tunneling current of $I_t = -0.08$ nA, (b) A 318 nm × 318 nm area of the Co(0001) surface, imaged under conditions for the Fischer-Tropsch (FT) synthesis of hydrocarbon molecules from a 1:2 mixture of CO and H_2 known as syngas. The total pressure is 1.2 bars, consisting of 200 mbar syngas and 1000 mbar Ar, and the temperature is 500 K. Imaged with a sample bias of $V_t = 1.05$ V and a tunneling current of $I_t = 0.15$ nA.

flow at a high pressure of 1.2 bars (panel (a)). The large-scale image of panel (b) shows the dynamic behavior of the atomic steps at this elevated temperature.[37] Note that the herringbone reconstruction that is clearly present in Figure 6 and characteristic for the clean Au(111) surface is absent in the images of Figure 7. We have not investigated systematically whether this lifting of the reconstruction is caused by the high-temperature exposure to the high O_2 pressure or by the presence of a trace impurity in the O_2 flow, such as water. We note that the images of Figure 7 have been obtained while three turbo-molecular pumps of the UHV system were running at full speed. Although this has introduced a minor vibrational signature in Figure 7(a), the effect is sufficiently modest, not to wash out the atomic resolution.

In Figure 8, we provide two STM images of catalytically more relevant situations. Panel (a) shows the Pt(110) surface at a temperature of 433 K in a flow of 1 bar of CO, taken in the course of an experiment dedicated to the catalytic oxidation of CO.[3,38–46] The distance between the atom rows shows that the CO has lifted the (1 × 2) reconstruction, characteristic of the clean surface. The atomic periodicity can be recognized vaguely in the atomic rows. The high temperature and the presence of the CO lead to rapid fluctuations in the position of the atomic step between the upper left and lower right parts of the image, which make the appearance of that step in the image extremely jagged. Similarly, large excursions can be recognized in the upper left corner of the image from a step with an average position to the left of the imaged area. In panel (b), we show the Co(0001) surface under conditions for the Fischer-Tropsch (FT) synthesis of hydrocarbon molecules from a flow at 200 mbar of a 1:2 ("syngas") mixture of CO and H_2 at a sample temperature of 500 K. The structures formed on the terraces and accumulating along the steps, have formed in the course of the FT reaction on this surface, and remain to be identified and further characterized.

STM tips require special attention when operating in catalytic conditions. Etched tungsten tips that traditionally perform well in ultrahigh vacuum are vulnerable for interaction with reactive gasses, such as water and oxygen. Tip oxidation compromises the imaging resolution under catalytically relevant conditions. Adsorption-enhanced diffusion of tip atoms can result in frequent changes in the shape and sharpness of the tip apex. In addition, the tip itself can be catalytically active and distort the reactivity measurements, although this effect is expected to be modest due to the small surface area and the lower temperature of the tip compared to the sample. Most results presented in this paper have been obtained with mechanically cut platinum-iridium tips. First tests with gold-coated metal tips give some hope that it may be possible to combine sharp, conductive tips with chemical inertness.

From the performance tests and the examples given in this section, we conclude that the ReactorSTM described in this paper fully meets the specifications given in Sec. III. It is the first STM capable of imaging catalytically interesting surfaces with atomic resolution under reaction conditions: high temperatures *and* high pressures of flowing gas mixtures. During imaging, the temperature of the catalyst, the flow rate, total pressure, and composition can all be changed over wide ranges, without the necessity to interrupt the imaging. Mass spectrometry of the gas that flows out of the reactor enables us to quantitatively correlate the catalytic performance of the model catalyst with the detailed structural information in the STM images, with a time resolution down to a few seconds.

VI. OUTLOOK

At present, the ReactorSTM is being used in the investigation of a growing variety of catalytic reaction systems. Examples are oxidation/reduction reaction, Fischer-Tropsch synthesis, and hydro-desulphurization. The observation in many of these cases of surface restructuring into high-gas-pressure-specific configurations should be taken as a justification *a posteriori* for the development of this special-purpose scanning tunneling microscopy setup for "the other side" of the pressure gap.

We close this paper by addressing several aspects that may further add to the performance of this microscope. The maximum sample temperature of 600 K and the maximum gas pressure of 6 bars are just within the range of industrial conditions. A higher operating temperature will require a different sealing material than Kalrez. We are in the process of replacing several of the components of the gas handling system in order to make the microscope suitable for a maximum pressure of 20 bars.

A highly relevant modification of our microscope that we are currently developing is that of a non-contact ReactorAFM version, as well as a version that combines the two functionalities, STM and nc-AFM. The two resulting forms of this microscope will enable us to also bridge the material gap and perform high-pressure, high-temperature observations on non-conductive surfaces, such as oxide supports and supported metal nanoparticles. This will take us beyond the geometry of extended, flat single-crystal metal surfaces and bring us closer to the geometry of practical catalysts.

ACKNOWLEDGMENTS

This project is financially supported by a Dutch Smart-Mix grant and the NIMIC partner organizations through NIMIC, a public-private partnership. The authors A. Ofitserov and G. J. C. van Baarle are employees of the company Leiden Probe Microscopy BV and the author J. W. M. Frenken is a shareholder in this company. One of LPM's products is a high-pressure STM setup that is strongly inspired by the research instrument that has been described in the present article.

[1]M. Bowker, *The Basis and Applications of Heterogeneous Catalysis* (Oxford Chemistry Primers, 1998).
[2]G. A. Somorjai, *Introduction to Surface Chemistry and Catalysis* (Wiley, New York, 1993).
[3]B. L. M. Hendriksen, M. F. Chang, M. A. J. Klik, and J. W. M. Frenken, Phys. Rev. Lett. **89**, 046101 (2002).
[4]M. D. Ackermann, T. M. Pedersen, B. L. M. Hendriksen, O. Robach, S. C. Bobaru, I. Popa, C. Quiros, H. Kim, B. Hammer, S. Ferrer, and J. W. M. Frenken, Phys. Rev. Lett. **95**, 255505 (2005).
[5]X. Su, P. S. Cremer, Y. Ron Shen, and G. A. Somorjai, J. Am. Chem. Soc. **119**, 3994 (1997).
[6]R. Westerström, J. Gustafson, A. Resta, A. Mikkelsen, J. N. Andersen, E. Lundgren, N. Serianr, F. Mittendorfer, M. Schmid, J. Klikovits, P. Varga, M. D. Ackermann, J. W. M. Frenken, N. Kasper, and A. Stierle, Phys. Rev. B **76**, 155410 (2007).
[7]H. Over and M. Muhler, Prog. Surf. Sci. **72**, 3 (2003).
[8]J. F. Creemer, S. Helveg, G. H. Hoveling, S. Ullmann, A. M. Molenbroek, P. M. Sarro, and H. W. Zandbergen, Ultramicroscopy **108**(9), 993 (2008).
[9]R. van Rijn, M. D. Ackermann, O. Balmes, T. Dufrance, H. Gonzalez, H. Isern, L. Petit, V. A. Sole, D. Wermeille, R. Felici, A. Geluk, E. De Kuyper, and J. W. M. Frenken, Rev. Sci. Instrum. **81**, 014101 (2010).
[10]P. B. Rasmussen, B. L. M. Hendriksen, H. Zeijlemaker, H. G. Ficke, and J. W. M. Frenken, Rev. Sci. Instrum. **69**, 3879 (1998).
[11]B. L. Weeks, C. Durkan, H. Kuramochi, M. E. Welland, and T. Rayment, Rev. Sci. Instrum. **71**(10), 3777 (2000).
[12]E. Lægsgaard, L. Österlund, P. Thostrup, P. B. Rasmussen, I. Stensgaard, and F. Besenbacher, Rev. Sci. Instrum. **72**(9), 3537 (2001).
[13]M. Rößler, P. Geng, and J. Wintterlin, Rev. Sci. Instrum. **76**(2), 023705 (2005).
[14]F. Tao, D. Tang, M. Salmeron, and G. A. Somorjai, Rev. Sci Instrum. **79**, 084101 (2008).
[15]S. B. Roobol, M. E. Cañas-Ventura, M. Bergman, M. A. van Spronsen, W. Onderwaater, P. C. van der Tuijn, R. Koehler, A. Ofitserov, G. J. C. van Baarle, and J. W. M. Frenken, "The ReactorAFM: Non-Contact Atomic Force Microscope operating under high-pressure and high temperature catalytic conditions" (unpublished).
[16]C. J. Chen, *Introduction to Scanning Tunneling Microscopy* (Oxford University Press, 1993).
[17]M. S. Hoogeman, D. Glastra van Loon, R. W. M. Loos, H. G. Ficke, E. de Haas, J. J. van der Linden, H. Zeijlemaker, L. Kuipers, M. F. Chang, M. A. J. Klik, and J. W. M. Frenken, Rev. Sci. Instrum. **69**, 2072 (1998).
[18]VG Scienta.
[19]UHV gate valve series 10, VAT Inc.
[20]VacIon Plus 150/300 StarCell Combination Pump, Agilent Technologies.
[21]Turbo-molecular pump TPH 261PC in combination with DUO 20 MC, Pfeiffer Vacuum.
[22]Pneumatic Vibration Isolators, Newport Corporation.
[23]Model IG70, OCI Vacuum Micro-engineering.
[24]Mini e-beam evaporator EGCO4, Oxford Applied Research.
[25]SpectaLEED, Omicron NanoTechnology GmbH.
[26]ALV, Leiden Probe Microscopy B.V.
[27]Focus 500 x-ray source, Phoibos 100 analyzer, 2D CCD detector, Flood gun FG15/40, SPECS Surface Nano Analysis GmbH.
[28]Custom part, DuPont.
[29]Zerodur, Schott.
[30]SmCo magnet, IBS Magnet.
[31]EBL #2, EBL Products.
[32]Corning Inc.
[33]Video Rate SPM Controller, Leiden Probe Microscopy B.V.
[34]M. Rost, L. Crama, P. Schakel, E. van Tol, G. van Velzen-Williams, C. Overgauw, H. ter Horst, H. Dekker, B. Okhuijsen, M. Seynen, A. Vijftigschild, P. Han, A. J. Katan, K. Schoots, R. Schumm, W. van Loo, T. H. Oosterkamp, and J. W. M. Frenken, Rev. Sci. Instrum. **76**, 053710 (2005).
[35]F-201CV EL-flow and P-702CV EL-press, Bronkhorst High-Tech B.V.
[36]T100 gas analyzer, Leiden Probe Microscopy B.V.
[37]L. Kuipers, M. S. Hoogeman, J. W. M. Frenken, and H. van Beijeren, Phys. Rev. B **52**(15), 11387 (1995).
[38]M. Kim, M. Bertram, M. Pollmann, A. von Oertzen, A. S. Mikhailov, H. H. Rotermund, and G. Ertl, Science **292**, 1357 (2001).
[39]S. Ladas, R. Imbihl, and G. Ertl, Surf. Sci. **197**, 153 (1988).
[40]H. P. Bonzel and R. Ku, J. Vac. Sci. Technol. **9**, 663 (1972).
[41]H. P. Bonzel and R. Ku, Surf. Sci. **33**, 91 (1972).
[42]A. von Oertzen, A. S. Mikhailov, H. H. Rotermund, and G. Ertl, J. Phys. Chem. B **102**, 4966 (1998).
[43]S. Ladas, R. Imbihl, and G. Ertl, Surf. Sci. **198**, 42 (1988).
[44]C. E. Wartnaby, A. Stuck, Y. Y. Yeo, and D. A. King, J. Chem. Phys. **102**, 1855 (1995).
[45]E. Vlieg, I. K. Robinson, and K. Kern, Surf. Sci. **233**, 248 (1990).
[46]Q. Ge and D. A. King, J. Chem. Phys. **111**, 9461 (1999).